International Journal of Scientific Research in Science and Technology
Print ISSN: 2395-6011 | Online ISSN: 2395-602X (www.ijsrst.com)
doi : https://doi.org/10.32628/IJSRST229680

Comparison of Several Methods for Automated Noise Measurements in Computed Tomography

Fitri Octaviany[1], Choirul Anam[1*], Heri Sutanto[1], Ariij Naufal[1]

[1]Department of Physics, Faculty of Sciences and Mathematics, Diponegoro University, Jl Soedarto SH, Tembalang, Semarang, 50275, Central Java, Indonesia

Article Info

Volume 9, Issue 6
Page Number : 566-573

Publication Issue

November-December-2022

Article History

Accepted : 05 Nov 2022
Published : 20 Dec 2022

ABSTRACT

Purpose: To compare the methods of automated noise measurement at the polyester resin (PESR) phantom images and clinical abdominal images.

Method: The PESR phantom was scanned with a Siemens SOMATOM Emotion 6 CT scanner for various tube voltages, i.e., 80, 110, and 130 kV. Noises from images of the PESR phantom and 27 clinical abdominal scans were automatically measured. The methods used for automatic measurements were methods proposed by Christianson et al (2015), Malkus et al (2017), and Anam et al (2019), respectively.

Results: Three methods of automatic noise measurements can distinguish the noise of the three tube voltages. The measured noises from three methods decrease with increasing tube voltage. It can also be seen that the highest noise in PESR phantom images is Christianson et al (2015) method, and the smallest noise is Malkus et al (2017) method. The highest noise in clinical abdominal images is Malkus et al (2017) method, and the smallest noise is Anam et al (2019) method.

Conclusion: The algorithms to automatically measure noises proposed by Christianson et al (2015), Malkus et al (2017), and Anam et al (2019) have been compared. Although the three methods can distinguish noise for different exposure factors, the magnitude of the noise from the three methods can vary. Until now there is no standard for automatic noise determination.

Keywords: CT scan, noise, automated noise, IndoQCT, tube voltage

I. INTRODUCTION

Computed tomography (CT) scan is a diagnostic modality that uses a combination of X-rays and computer to provide excellent images in axial, sagittal, and coronal planes [1]. CT images are used to diagnose diseases, to perform screening purposes, and to plan radiotherapy procedure [2]. CT is used because it has

Copyright: © the author(s), publisher and licensee Technoscience Academy. This is an open-access article distributed under the terms of the Creative Commons Attribution Non-Commercial License, which permits unrestricted non-commercial use, distribution, and reproduction in any medium, provided the original work is properly cited

several advantages, such as it produces high-quality images with fast acquisition times and relatively low cost [3]. There are several input parameters of CT to obtain optimal image quality, such as tube voltage, tube current, rotation time, slice thickness, field of view, gantry tilt, filter, and reconstruction algorithm [4].

To maintain CT image quality, it is necessary to perform quality assurance (QA) procedures regularly. Good image quality provides useful clinical information to radiologists to accurately diagnose abnormalities within patient [5]. One of the important image quality parameters in CT is noise level and noise texture [6-8].

Noise is a fluctuation in the pixel value of an image in a homogeneous area. Pixel value in CT is expressed as CT number. CT number indicates value of the X-ray absorption coefficient on an object that has been calibration with water and it expressed in Hounsfield unit (HU). Noise is usually measured using the standard deviation (SD) of the pixel values within homogeneous area. When SD is high, the noise also gets higher [8-10]. Several factors affect noise, such as tube voltage (kVp), tube current (mA), tube rotation speed (s), pitch, slice thickness, and reconstruction method [9,11].

Determining noise is usually measured manually using the region of interest (ROI) in a homogeneous area [12-15]. Measuring noise is generally carried out in the phantom's images and not in clinical patient images. It is noted that for dose optimization, measuring dose and noise in phantoms are not sufficient, therefore measuring of the noise in clinical patient image is needed. However, manual noise measurement in patient images is impractical in busy CT center. In addition, manual noise measurement tends to generate variability among medical staff because deciding the ROI location at the most homogenous is subjective. Therefore, an automated method of measuring noise is needed. Currently, several methods for measuring noise automatically from patient images have been proposed, such as by Christianson et al (2015) [16], Malkus et al (2017) [17], and Anam et al (2019) [18].

Christianson et al [16] developed an automated method for measuring noise on abdominal-thoracic phantom and abdominal CT images. This method uses the global noise index (GNI) meaning that noise is identified as the most frequent SD from the SD map of the soft tissues. The method might not work well on non-abdominal images because the soft tissue does not cover a large area. Subsequently, Malkus et al [17] proposed an automated method that is able to measure noise in other than abdominal images, i.e. by the most frequent SD from SD map of the air surrounding the patient. It is reported that the method can be accurately used as a substitute for noise inside the patient. Another method was proposed by Anam et al [18] which the proposed algorithm can be implemented on CT images of all body parts. Noise is automatically measured as the minimum magnitude obtained from the SD map within the patient images [18,19].

However, there is no study to compare the available automated noise algorithms for determining noise measurements on the same image. This study aims to compare algorithms of automated noise measurements on the images of polyester resin (PESR) phantom with a diameter of 32 cm and clinical abdominal scans.

II. METHODS AND MATERIAL

A. Automated noise measurement

All images generated from the scanning process were saved in the Digital Imaging and Communications in Medicine (DICOM) format. Then, automated noise measurements were carried out with various measurement algorithms (Christianson et al [16], Malkus et al [17], and Anam et al [18] methods) already integrated in IndoQCT [20]. A graphical user interface (GUI) to automatically measure noise measurement is shown in Figure 1. GUI provided kernel settings used in each algorithm.

B. Christianson et al (2015) method [16]

Automated noise measurement by Christianson et al [16] used the global noise index (GNI) method. To obtain the GNI, soft tissue of the image was segmented with the threshold from 0 to +100 HU. Furthermore, the SD map was developed using of sliding window kernel that covers the entire image according to soft tissue mask. The SD in every sliding window kernel position was calculated using equation (1).

$$SD(x,y) = \sqrt{\frac{1}{n \times n}\sum_{i=1}^{n \times n}(I_{b,i} - \bar{I_b})^2} \qquad (1)$$

where n × n is the size of the sliding window kernel.

The histogram was made from the SD map data. GNI was determined by identifying the SD at the histogram peaks corresponding to a homogeneous soft tissue. Figure 2 shows the automated noise measurement steps proposed by Christianson et al [16].

C. Malkus et al (2017) method [17]

In this method, the SD map was obtained from the air outside the patient. The air region was obtained by automated segmentation. Dilation process was made on the segmented image to enlarge the area of patient. Next, the image was converted to the negative image. The original image was masked with this negative image. After that, the SD map was created in the area of air outside the patient. The GNI was obtained from air SD map at the highest frequency as in the previous method. Figure 3 shows the automated noise measurement steps by Malkus et al [17].

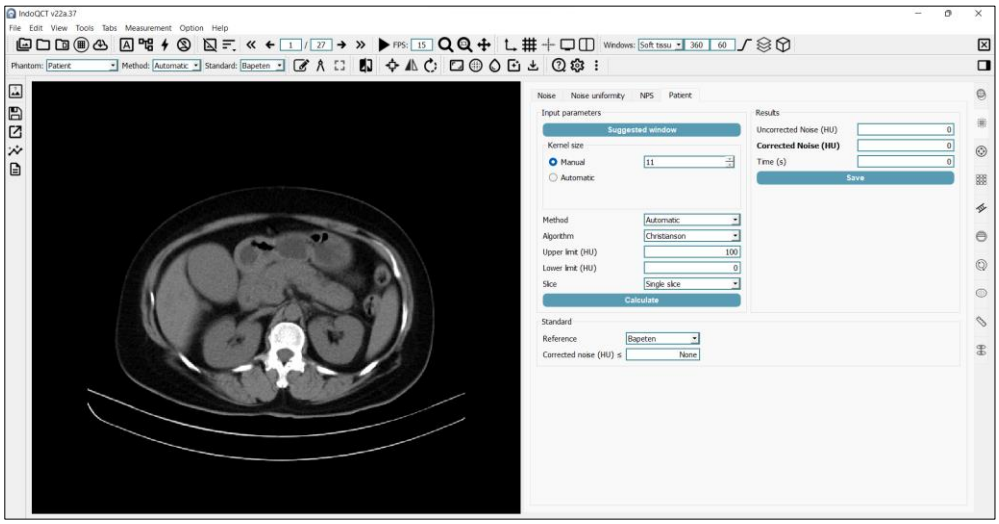

Figure 1. GUI for automated noise measurements using three different methods.

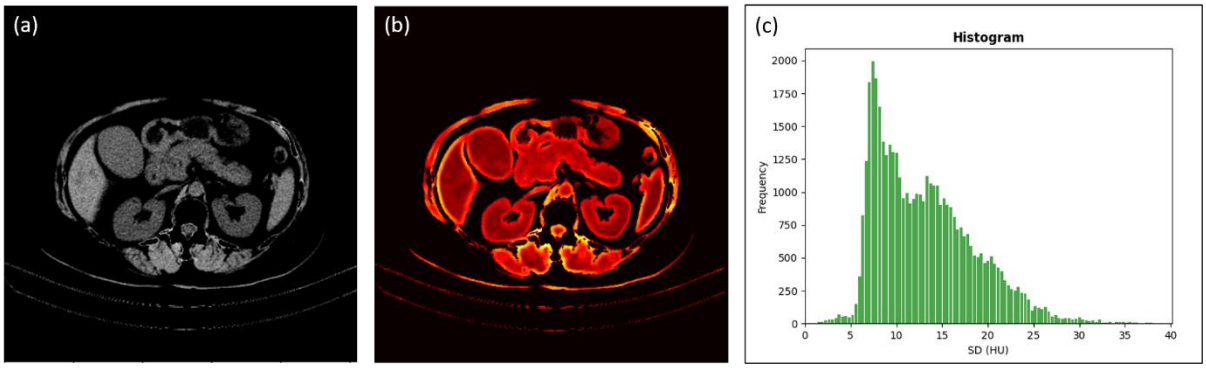

Figure 2. Steps of automated noise measurement by Christianson et al [16], (a) original abdominal image, (b) SD map within soft tissue, and (c) peak histogram showing noise

D. Anam et al (2019) method

Automated noise measurement by Anam et al [18] was done by segmentation of all part of patient image. The SD map then developed by calculating the SD value for each pixel with a sliding window operation performed using a specific kernel size. Then, estimate the noise was determined as the smallest SD from the SD map. The position of the smallest SD was determined by equation (2).

$$[X_{min}, Y_{min}] = argmin\,(SD_n) \qquad (2)$$

The example of an automated noise calculation process using the Anam et al [18] method is shown in Figure 4.

E. Phantom and patient images

In this study, we measure noise images of phantom and patients. The phantom was made from the polyester resin (PESR) and methyl ethyl ketone peroxide (MEKP) as catalysts [22-24]. The phantom was with a thickness of 15 cm and diameter of 32 cm is shown in Figure 5. The phantom was scanned with Siemens Somatom Emotion 6 CT scanner with various tube voltages, i.e., 80, 110, and 130 kVp. In each phantom image dataset, 5 slices were selected for examination. Meanwhile, one slice abdominal image from 27 patients were retrospectively analyzed. The exposure parameters used are shown in Table 1.

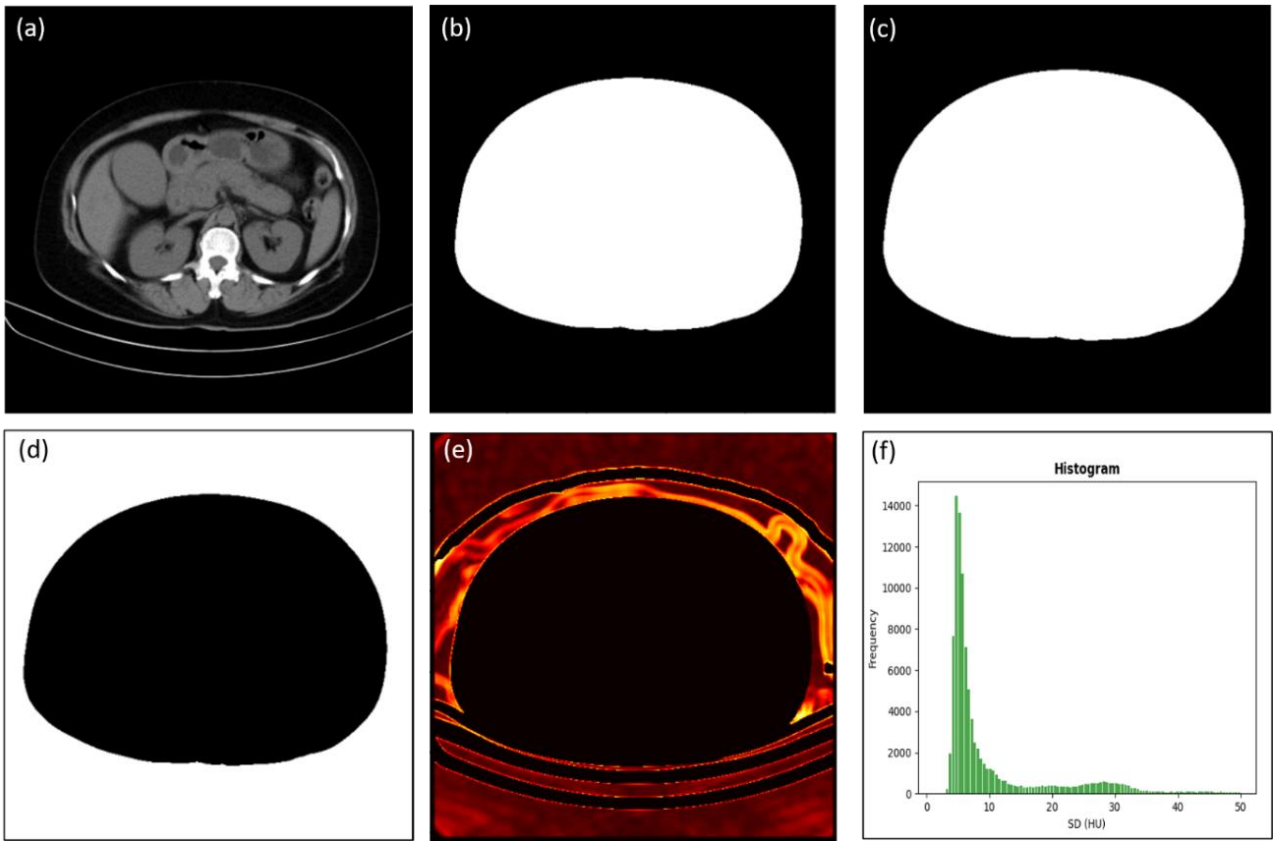

Figure 3. Steps of automated noise measurement by Malkus et al [17] on abdominal images, (a) original abdominal image, (b) patient's segmentation image, (c) dilation of segmented image, (d) negative image, (e) SD map in the air region, and (f) histogram of the SD map for areas in the air region.

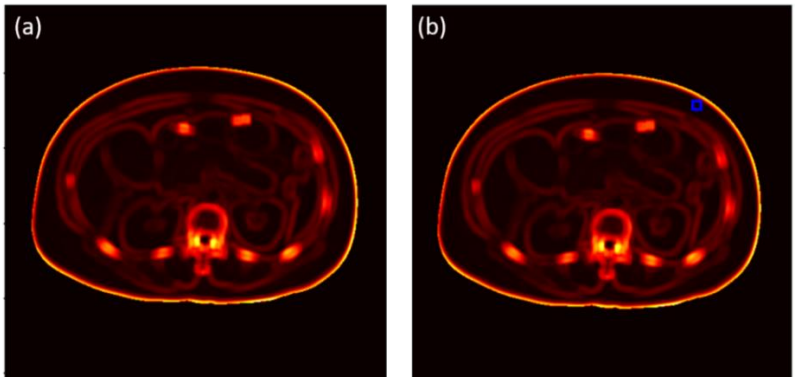

Figure 4. Automated noise measurement by Anam et al [18] method on abdominal image, (a) SD map images, and (b) ROI in the most homogeneous image area (smallest value from SD map)

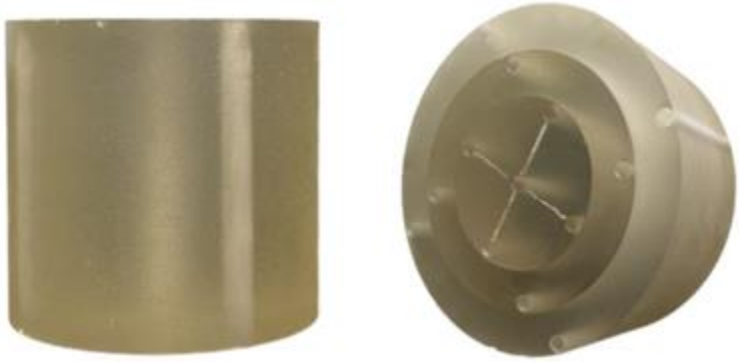

Figure 5. The PESR phantom with a diameter of 32 cm.

Table 1. Scan parameter

Scan parameters	Phantom images	Clinical images
Scanner	Siemens Somatom Emotion 6	Siemens Somatom Emotion 6
Tube voltage (kV)	80, 110, and 130	130
Slice thickness (mm)	1	10
Tube current (mA)	TCM	TCM
Rotation time (ms)	600	600
FOV (mm)	500	253 – 370
Pitch	0.6	0.6
Scan protocol	Abdomen routine	Abdomen routine

III.RESULTS AND DISCUSSION

Figure 6 shows the comparison of noises in the PESR phantom images measured using Christianson et al [16], Malkus et al [17], and Anam et al [18] methods for tube voltages of 80, 110, and 130 kV. Three methods can distinguish the noise of the three tube voltages. The noise in PESR phantom images and abdominal images has a dependence on tube voltage. The measured noise decreases with increasing tube voltage. It can also be seen that the highest noise in PESR phantom images is Christianson et al [16] method, and the smallest noise is Malkus et al [17] method.

Figure 7 shows the box-plots of noise from abdominal images for Christianson et al [16], Malkus et al [17], and Anam et al [18] methods. It shows that the highest noise is in the Malkus et al [17] method, then Christianson et al [16] method, and the lowest noise is using Anam et al [18] method.

Table 2 shows the calculation time for each method. It can be seen that Anam et al [18] method has the shortest time compared to the other methods, and Christianson et al [16] method has the longest time compared to the other methods.

Manual noise measurement in CT images is subjective, since it is affected by the ROI positioning by medical staff. Therefore, more objective and effective measurement is needed. Several methods for automated noise measurement have been proposed (Christianson et al [16], Malkus et al [17], and Anam et al [18]). The current study compares noises measured using three methods of the PESR phantom images scanned with three different tube voltages and noises of 27 abdominal images.

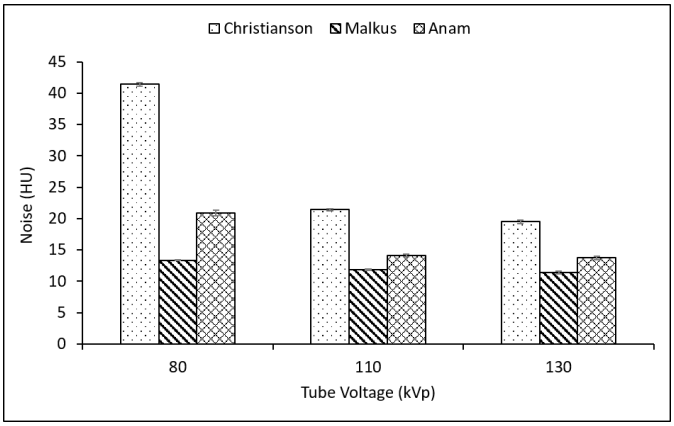

Figure 6. Graphs of noise in PESR phantom at the three methods for various voltages

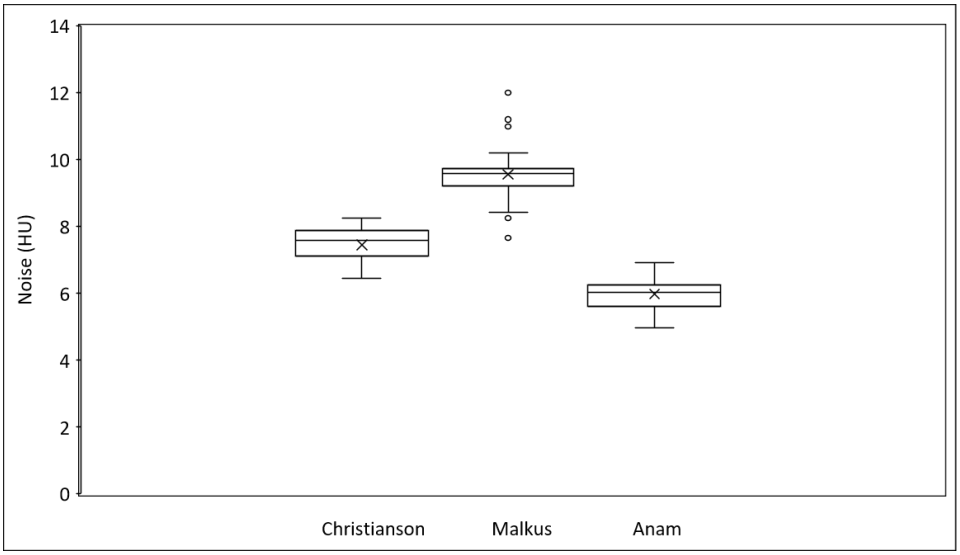

Figure 7. The relationship between the noise from the proposed method in the abdominal image. The box-and-whisker graph shows the median and 25th and 75th percentiles of each method. Outliers are indicated by the ○ sign that exceeds 1.5 times interquartile length.

Table 2. Time required for noise measurements

Images	Processing time (s)		
	Christianson et al (2015)	Malkus et al (2017)	Anam et al (2019)
PESR phantom at 80 kV	6.38	5.28	2.55
PESR phantom at 110 kV	6.14	4.87	2.41
PESR phantom at 130 kV	6.21	4.95	2.45
Abdomen	6.28	3.64	3.35

We found that measured noise has an inversely proportional with tube voltage. As shown in Figure 6, the noise decreases with increasing the tube voltage from 80 to 130 kV. All of the automatic noise measurement methods show this trend. This phenomenon of noise dependency on tube voltage is well-understood [24,25]. The three algorithms (Christianson et al [16], Malkus et al [17], and Anam et al [18]) have indeed reported that they can detect changes in noise due to changes in exposure factors such as tube current, tube voltage, phantom diameter, and the reconstruction algorithm. Thus, the results of this study have confirmed that automatic noise measurement can detect changes in noise due to changes in exposure factors, such as tube voltage.

Figure 6 shows the noise in the PESR phantom image using the Christianson et al method [16] gets the highest noise. However, for abdominal images, the highest noise is using the Malkus et al [17] method as shown in Figure 7. The smallest noise in PESR phantom images is Malkus et al [17] method, in clinical abdominal images is Anam et al [18] method. Each algorithm has advantages and disadvantages. Until now there is no standard in this automatic noise calculation. Therefore, further studies with a larger number of images need to be carried out.

The speed of the calculation process is one of the important factors to determine the usability value of the algorithms. The differences in the speed of noise measurement in Christianson et al [16], Malkus et al [17], and Anam et al [18] method are around 7, 6, and 4 seconds, respectively.

IV. CONCLUSION

The algorithms to automatically measure noises proposed by Christianson et al (2015) [16], Malkus et al (2017) [17], and Anam et al (2019) [18] have been compared. It is found that three methods of automatic noise measurements can distinguish the noise of the three tube voltages. The measured noises from three methods decrease with increasing tube voltage. The magnitude of the noise from the three methods can vary. The highest noise in PESR phantom images is Christianson et al (2015) [16] method, and in clinical abdominal images is Malkus et al (2017) [17] method. The smallest noise in PESR phantom images is Malkus et al (2017) [17] method, in clinical abdominal images is Anam et al (2019) [18] method. Until now there is no standard for automatic noise determination.

V. ACKNOWLEDGEMENTS

This work was funded by the Riset Publikasi International Bereputasi Tinggi (RPIBT), Diponegoro University, No. 569-187/UN7.D2/PP/VII/2022.

VI. REFERENCES

[1] Lampignano J & Kendrick LE. *Bontrager's Textbook of Radiographic Positioning and Related Anatomy 9th Edition*. Elsevier Health Sciences; 2017.

[2] Vega-Woo N. Evaluation of radiation exposure from computed tomography of the head. *J Radiol Nursing*. 2018;37(4):260-267.

[3] Roa AM, Andersen HK, Martinsen AC. CT image quality over time: comparison of image quality for six different CT scanners over a six-year period. *J Appl Clin Med Phys*. 2015;16(2):4972.

[4] Okada DR, & Blankstein R. Digital image processing for medical applications. *Perspectives in Biology and Medicine*. 2009;52(4):617-623.

[5] Zarb F, Rainford L, & McEntee MF. Image quality assessment tools for optimization of CT images. *Radiography*. 2010;16(2):147-153.

[6] Verdun FR, Meuli RA, Bucher G, Noel A, Stines J, Schnyder P, & Valley JF. Dose and image quality characterization of CT units. *Radiat Prot Dosim*. 200;90(1-2):193-196

[7] Seeram E. *Computed Tomography-E-Book: Physical Principles, Clinical Applications, and Quality Control*. Elsevier Health Sciences; 2015.

[8] Goldman LW. Principles of CT: radiation dose and image quality. *J Nucl Med Technol*. 2007;35(4):213-228.

[9] Bushberg JT & Boone JM. *The Essential Physics of Medical Imaging*. Lippincott Williams & Wilkins;

2011.

[10] Khoramian D, Sistani S, Firouzjah RA. Assessment and comparison of radiation dose and image quality in multi-detector CT scanners in non-contrast head and neck examinations. *Pol J Radiol*. 2019;84:e61-e67.

[11] Solomon JB, Li X, Samei E. Relating noise to image quality indicators in CT examinations with tube current modulation. *AJR Am J Roentgenol*. 2013;200(3):592-600.

[12] Primak AN, McCollough CH, Bruesewitz MR, Zhang J, Fletcher JG. Relationship between noise, dose, and pitch in cardiac multi-detector row CT. *Radiographics*. 2006;26(6):1785-1794.

[13] Kamezawa H, Arimura H, Shirieda K, Kameda N, Ohki M. Feasibility of patient dose reduction based on various noise suppression filters for cone-beam computed tomography in an image-guided patient positioning system. *Phys Med Biol*. 2016;61(9):3609-3636.

[14] Dodge CT, Tamm EP, Cody DD, et al. Performance evaluation of iterative reconstruction algorithms for achieving CT radiation dose reduction - a phantom study. *J Appl Clin Med Phys*. 2016;17(2):511-531.

[15] Hussain FA, Mail N, Shamy AM, Suliman A, Saoudi A. A qualitative and quantitative analysis of radiation dose and image quality of computed tomography images using adaptive statistical iterative reconstruction. *J Appl Clin Med Phys*. 2016;17(3):419-432.

[16] Christianson O, Winslow J, Frush DP, Samei E. Automated Technique to Measure Noise in Clinical CT Examinations. *AJR Am J Roentgenol*. 2015;205(1):W93-W99.

[17] Malkus A, Szczykutowicz TP. A method to extract image noise level from patient images in CT. *Med Phys*. 2017;44(6):2173-2184.

[18] Anam C, Budi WS, Adi K, et al. Assessment of patient dose and noise level of clinical CT images: automated measurements. *J Radiol Prot*. 2019;39(3):783-793.

[19] Anam C, Arif I, Haryanto F, et al. An Improved Method of Automated Noise Measurement System in CT Images. *J Biomed Phys Eng*. 2021;11(2):163-174.

[20] Anam C, Naufal A, Fujibuchi T, Matsubara K, Dougherty G. Automated development of the contrast-detail curve based on statistical low-contrast detectability in CT images. *J Appl Clin Med Phys*. 2022;23(9):e13719.

[21] Hilmawati R, Sutanto H, Anam C, Arifin Z, Asiah RH, Soedarsono JW. Development of a head CT dose index (CTDI) phantom based on polyester resin and methyl ethyl ketone peroxide (MEKP): a preliminary study. *J Radiol Prot*. 2020;40(2):544-553.

[22] Asiah R, Sutanto H, Anam C, Arifin Z, Bahrudin B, & Hilmawati, R. Development of in-house head computed tomography dose index phantoms based on polyester-resin materials. *Iran J Med Phys*. 2021;18(4):255-262.

[23] Dio P, Anam C, Hidayanto E, et al. Evaluation of radiation dose accuracy calculated using IndoseCT software with direct measurement on polyester-resin phantoms. *Radiat Phys Chem*. 2022;201:110473

[24] Anam C, Haryanto F, Widita R, & Arif I. New noise reduction method for reducing CT scan dose: Combining Wiener filtering and edge detection algorithm. In *AIP Conference Proceedings* 2015;1677(1):040004

[25] Choi HR, Kim RE, Heo CW, Kim CW, Yoo MS, & Lee Y. Optimization of dose and image quality using self-produced phantom with various diameters in pediatric abdominal CT scan. *Optik*. 2018;168:54-60.

Cite this article as :

Fitri Octaviany, Choirul Anam, Heri Sutanto, Ariij Naufal, "Comparison of Several Methods for Automated Noise Measurements in Computed Tomography", International Journal of Scientific Research in Science and Technology (IJSRST), Online ISSN : 2395-602X, Print ISSN : 2395-6011, Volume 9 Issue 6, pp. 566-573, November-December 2022.
Available at doi : https://doi.org/10.32628/IJSRST229680
Journal URL : https://ijsrst.com/IJSRST229680